

# From powder to complex-shaped NiTi structures by selective laser melting

Therese Bormann<sup>1,2</sup>, Ralf Schumacher<sup>1</sup>, Bert Müller<sup>2</sup> and Michael de Wild<sup>1</sup>

<sup>1</sup> Institute for Medical and Analytical Technologies, University of Applied Sciences Northwestern Switzerland, Gründenstrasse 40, 4132 Muttenz, Switzerland.

<sup>2</sup> Biomaterials Science Center, University of Basel, c/o University Hospital, 4031 Basel, Switzerland.

## Abstract

Selective laser melting (SLM) is an additive manufacturing technique, which allows the fabrication of a wide variety of three-dimensional geometries by laser-induced melting of powder layers. Complex shapes including porous parts and filigree lattice structures can thereby be created in a single processing step directly from powder. Specimens from the biocompatible shape memory alloy NiTi were produced by means of a SLM system. These specimens exhibit the characteristic pseudoelastic behaviour as well as the one-way shape memory effect [1]. In addition, by varying the processing parameters we locally controlled the phase transition temperatures. Investigations of the specimens' microstructure using optical microscopy reveal the processing route of the laser manufacturing and show an anisotropic microstructure. In sum, the SLM-process is a promising method to build functional medical implants and scaffolds for tissue engineering.

## Introduction

NiTi, an FDA-approved biocompatible alloy, exhibits extraordinary properties including pseudoelasticity, shape memory effect and damping capacities. These properties are based on a reversible martensitic phase transformation between a high-temperature cubic crystalline phase (austenite) and a low-temperature monoclinic crystalline phase (martensite). The phase transformation is triggered either by thermal or mechanical stimuli. The phase transformation may be well adjusted between  $-100\text{ }^{\circ}\text{C}$  to  $150\text{ }^{\circ}\text{C}$  by tailoring the Ni to Ti ratio. A detailed description of this relationship can be found in literature [2]. As this temperature range includes the body temperature, it is implied that the effects are well suited for medical applications. The SLM fabrication process is schematically shown in Fig. 1. A focused laser beam transmits the contour information of the desired part slice-by-slice into a bed of metallic powder, which locally melts and consolidates. This allows the fabrication of complex-shaped parts with a predefined three-dimensional architecture. Processing NiTi by selective laser melting (SLM), we produced filigree lattice structures with strut sizes down to  $200\text{ }\mu\text{m}$  [3]. As we show in this communication, processing of NiTi by SLM allows also global or local tailoring of mechanical and thermo-mechanical properties. In this way pseudoelastic and pseudoplastic behavior can be combined in one NiTi part. SLM produced NiTi implants could therefore exhibit pseudoelastic shock-absorbing regions, as well as pseudoplastic regions with a reduced Young's modulus.

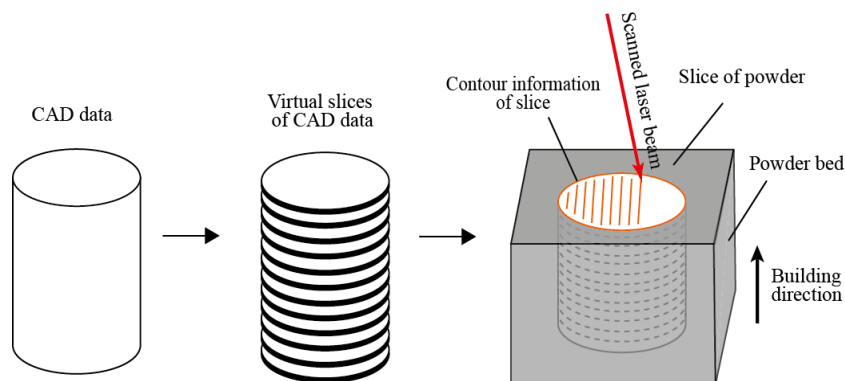


Fig. 1: Scheme of the SLM fabrication process.

## Experimental procedures

Cylinders and scaffolds as displayed in Fig. 2, were produced by means of the SLM 100 (SLM-solutions, Lübeck, Germany) from pre-alloyed NiTi-powder (MEMRY GmbH, Weil am Rhein, Germany) with a nominal Ni-content of 55.96 wt.-%. After correction about the oxygen and carbon content as described by Frenzel et al. [2], this corresponds to a Ni-content of 51.05 at.-%. The SLM machine is equipped with a continuous wave Ytterbium fibre laser with a maximum power of 100 W. For specimen fabrication, the laser power was varied between 60 and 95 W and the scanning velocity between 122 and 171 mm/s. This choice of processing parameters resulted in energy inputs of 60, 70, 84, 100 and  $130\text{ J/mm}^3$  [1]. The phase transition temperatures (austenite start ( $A_s$ ), austenite peak ( $A_p$ ), austenite finish ( $A_f$ ), martensite start ( $M_s$ ), martensite peak ( $M_p$ ) and

martensite finish ( $M_f$ ) were determined using differential scanning calorimetry (DSC 30, Mettler-Toledo) with a heating rate of 10 K/min. The oxygen content of NiTi cylinders built at 60, 70, 84 and 100 J/mm<sup>3</sup> and the powder was measured by inert gas fusion method (Galileo G8, Bruker, Karlsruhe, Germany). Mechanical properties of the scaffolds were determined at room temperature by compression tests using a universal testing machine (Z100, Zwick/Roell, Ulm, Germany). The strain was measured via the machine traverse displacement. The preparation of the specimens for microstructure characterization included cutting, embedding, grinding, mechanical polishing, electro-polishing and etching. The electrolyte for electro-polishing consisted of 3 M H<sub>2</sub>SO<sub>4</sub> in 1:1 ethanol-methanol. Etching was carried out according to the protocol described by Escher et al. [5].

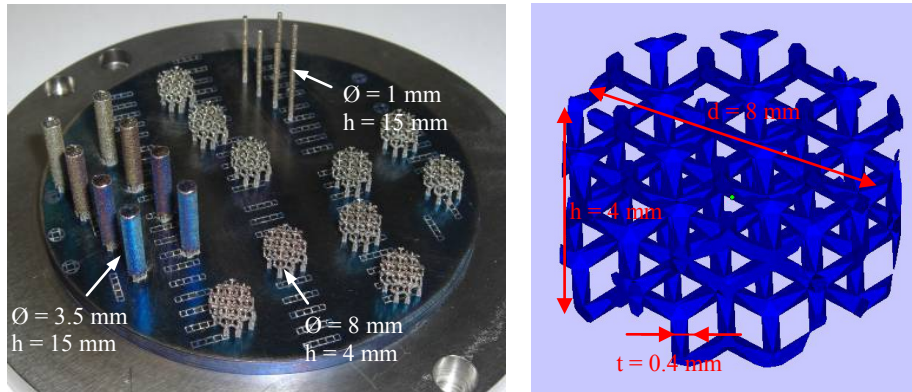


Fig. 2: Left: Photograph of NiTi cylinders and scaffolds, attached to the support structures on the SLM building platform. Right: CAD model of the scaffolds.

## Results and discussion

In SLM NiTi cylinders, the energy input was varied between 60 and 100 J/mm<sup>3</sup>. The increase of the energy input resulted in increased phase transition temperatures of up to 50 K [4]. By applying different processing parameters during the production in single specimen, gradients in the transition temperatures were induced, as exemplarily shown by the data in Tab. 1. The reason behind these altered transition temperatures is the preferential evaporation of Ni from the alloy during the processing, as the transition temperatures depend strongly on the Ni to Ti ratio [2]. In the upper part of the cylinder, which has the higher transition temperatures and was produced at 100 J/mm<sup>3</sup>, Ni should have preferentially been evaporated. Frenzel et al. provided a relationship between the Ni-content and the transition temperatures [2]. Applying these data, a difference in the Ni-content of about (0.11 ± 0.06) at.-% between the two parts of the cylinder was found. As the SLM-produced NiTi-parts show an enlarged temperature range for the transition temperature with respect to the raw material, we used the thermodynamic equilibrium temperature  $T_0$  for the calculations, which was described by Tong and Wayman [6]. It can be obtained from

$$T_0(x_{Ni}) = (M_s(x_{Ni}) + A_f(x_{Ni}))/2.$$

Nevertheless, it is difficult for our SLM-produced specimens to conclude on the absolute Ni to Ti ratio from the transition temperatures as the broad temperature range for the phase transition might be caused by inhomogeneous Ni and Ti distributions within the specimens. In addition, the raw material used (prior to atomization) does not exactly match the relationships used for the calculations.

Considering the impurity uptake, we found increased oxygen contents from (0.075 ± 0.004) wt.-% in the powder to (0.092 ± 0.009) wt.-% in the SLM fabricated specimens. The oxygen uptake is independent of the applied energy density and therefore not responsible for the shift in the phase transition temperatures.

In contrary to the dependence of the phase transition temperature on energy input in dense NiTi cylinders, in filigree scaffolds, the variation of the energy input between 60 J/mm<sup>3</sup> and 130 J/mm<sup>3</sup> did not change the phase transition temperatures. All scaffolds exhibited austenite peak temperatures between -36 °C and -24 °C, as shown in Fig. 3. Still, the increased energy input leads to a gain in the scaffold mass of about 100 mg (see Fig. 3). This mass increase is explained by the enlarged zone of powder consolidation, which gives rise to thicker lattice struts [7]. This behavior resulted in higher Young's moduli and maximal compression forces (see Fig. 4). The scaffolds exhibit pseudoelastic behavior directly after the SLM fabrication, i.e. without additional heat treatments (Fig. 5). We detected a recovery of the scaffold deformation of up to 5%, as exemplarily shown in Fig. 5. The loading-unloading curve displayed in Fig. 5 was detected using a scaffold built at 100 J/mm<sup>3</sup>.

Fig. 6 illustrates an anisotropic microstructure in SLM-built NiTi. The NiTi cylinders contain columnar grains with lengths up to several hundred micrometers (Fig. 6a). This anisotropy is caused by epitaxial grain growth along the heat transfer, which corresponds to the building direction [8]. Perpendicular to the building direction,

the grains reach widths of up to 150  $\mu\text{m}$  (see Fig. 6b). Their arrangement refers to the alternating laser route with a vector spacing of 120  $\mu\text{m}$ , as indicated.

Tab. 1: Different transition temperatures in the upper and lower part of dense NiTi cylinders depending on the applied energy density.

Energy input [ $\text{J}/\text{mm}^3$ ]	$A_s$ [ $^{\circ}\text{C}$ ]	$A_p$ [ $^{\circ}\text{C}$ ]	$A_f$ [ $^{\circ}\text{C}$ ]	$M_s$ [ $^{\circ}\text{C}$ ]	$M_p$ [ $^{\circ}\text{C}$ ]	$M_f$ [ $^{\circ}\text{C}$ ]	$T_0$ [ $^{\circ}\text{C}$ ]
100	$-23 \pm 2$	$20 \pm 4$	$41 \pm 2$	$19 \pm 4$	$-5 \pm 3$	$-47 \pm 9$	$30 \pm 4.5$
60	$-34 \pm 1$	$-5 \pm 1$	$27 \pm 1$	$12 \pm 1$	$-12 \pm 1$	$-80 \pm 6$	$19.5 \pm 1.5$

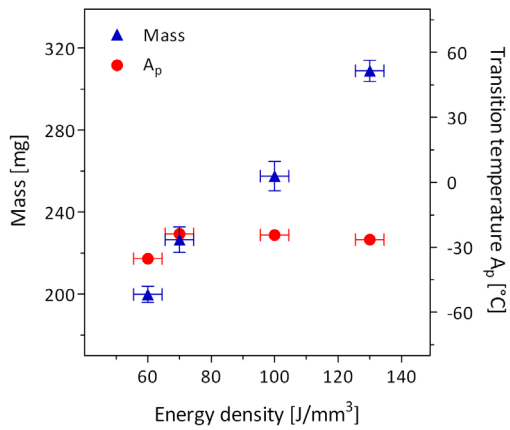


Fig. 3: Mass and austenite peak temperature of scaffolds built at different energy densities.

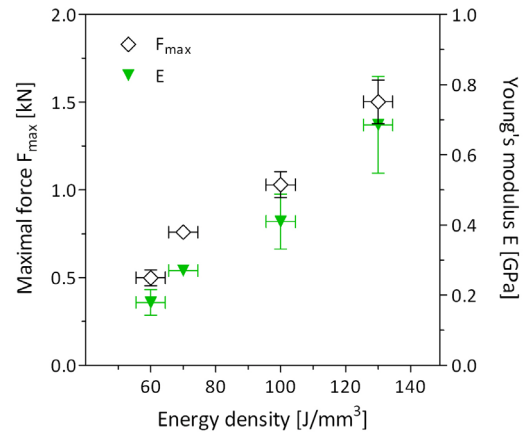


Fig. 4: Maximal force and Young's modulus of NiTi scaffolds built at different energy densities.

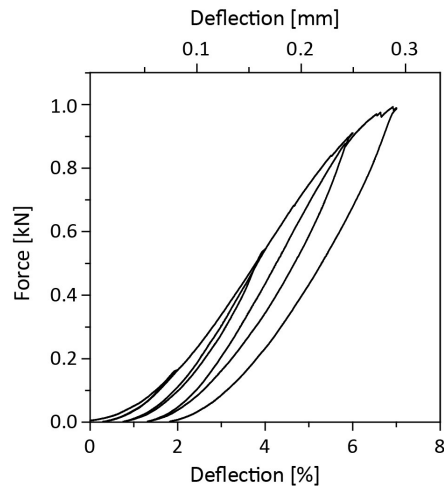


Fig. 5: The cyclic loading of a NiTi scaffold built at 100  $\text{J}/\text{mm}^3$  elucidates the pseudoelastic behavior.

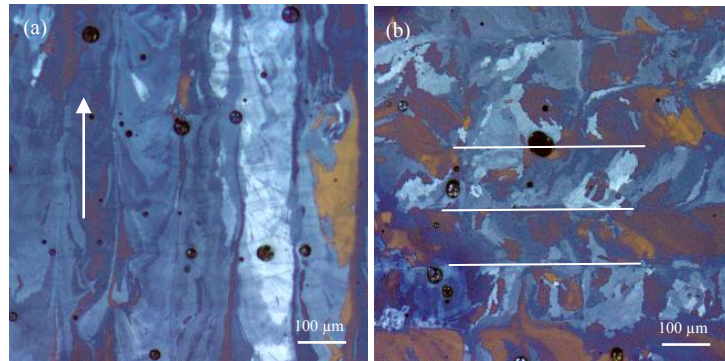


Fig. 6: The metallographic sections show the microstructure of SLM built NiTi cylinders: Fig. 6a displays the elongated grains along the building direction (indicated by arrow). Fig. 6b reveals the grain arrangement in the cross section, which refers to the pathway of the laser vectors (indicated by lines).

### Summary and conclusions

The application of SLM allows producing complex-shaped parts, such as filigree scaffolds, with pseudoelastic properties. Furthermore, the mechanical properties of the scaffolds are altered controlling the process parameters. In compact NiTi-cylinders, one can induce local changes of the transition temperatures, leading to functionally graded specimens. In this manner, NiTi systems can be realized, which permit the fabrication of medical implants with a sophisticated biomimetic performance.

### Acknowledgement

We sincerely thank MEMRY GmbH for powder- and knowledge-supply. Furthermore, the multi-disciplinary team gratefully acknowledges the financial support of the Swiss National Science Foundation within the program NRP 62 ‘Smart Materials’.

### References

- [1] T. Bormann, S. Friess, M. de Wild, R. Schumacher, G. Schulz and B. Müller, Determination of strain fields in porous shape memory alloys using micro computed tomography, *Proc. of SPIE*, Vol. 7804, 2010, 78041M.
- [2] J. Frenzel, E.P. George, A. Dlouhy, C. Somsen, M.X.F. Wagner and G. Eggeler, Influence of Ni on martensitic transformations in NiTi shape memory alloys, *Acta Mater.*, 58, 2010, p. 3444 – 3458.
- [3] T. Bormann, R. Schumacher, B. Müller and M. de Wild, Fabricating NiTi shape memory scaffolds by selective laser melting, *Eur. Cells Mater.*, 22(Suppl. 1), 2011, p. 12.
- [4] T. Bormann, R. Schumacher, B. Müller, M. Mertmann and M. de Wild, Tailoring selective laser melting process parameters for NiTi implants, *J. Mater. Eng. Perform.*, in press
- [5] K. Escher and M. Huehner, Metallographical preparation of NiTi shape memory alloys, *Prakt. Metallogr.*, 27(5), 1990, p. 231-235.
- [6] H.C. Tong and C.M. Wayman, Characteristic temperatures and other properties of thermoelastic martensites, *Acta Metall.*, 22(7), 1974, p. 887-896.
- [7] I. Yadroitsev, A. Gusarov, I. Yadroitsava and I. Smurov, Single track formation in selective laser melting of metal powders, *J. Mater. Process. Technol.*, 210(12), 2010, p. 1624-1631.
- [8] L. Thijs, F. Verhaeghe, T. Craeghs, J.V. Humbeeck and J.P. Kruth, A study of the microstructural evolution during selective laser melting of Ti-6Al-4V, *Acta Mater.*, 58(9), 2009, p. 3303-3312.